RadioGraphics

Teeth: What Radiologists Should Know[1]

Meir H. Scheinfeld, MD, PhD • Keivan Shifteh, MD • Laura L. Avery, MD
Harry Dym, DDS • R. Joshua Dym, MD

CME FEATURE

See www.rsna.org/education/search/RG

LEARNING OBJECTIVES FOR TEST 3

After completing this journal-based CME activity, participants will be able to:

- Describe the anatomy of the tooth and its support structures.
- Discuss the imaging findings of dental restorations.
- List common inflammatory conditions that affect the teeth.

TEACHING POINTS

See last page

Disease of the teeth and their support structures is common and frequently seen at imaging of the head and neck. Recognition of dental disease by the interpreting radiologist has the potential to alter the course of patient care, such as when periapical disease is identified as the cause of sinusitis or pericoronitis is identified as the cause of deep neck infection. Furthermore, incidental recognition of carious lesions in both children and adults who are undergoing CT for other reasons may alert the patient and care team of the need for a dental consultation. In fact, most of the images of dental and periodontal conditions that are used in this article were obtained from CT studies that were performed to investigate other problems. Familiarity with the imaging appearance of common dental conditions, such as hyperdontia and hypodontia, tooth trauma, periodontal disease, caries, periapical disease, odontogenic sinusitis, and deep neck infections, allows the radiologist to render a timely, confident, and specific diagnosis of dental abnormalities, even when such findings are unexpected.

Abbreviations: ADA = American Dental Association, FDI = Federation Dentaire Internationale, 3D = three-dimensional

RadioGraphics 2012; 32:1927–1944 • **Published online** 10.1148/rg.327125717 • **Content Codes:** CT HN NR

[1]From the Department of Radiology, Divisions of Emergency Radiology (M.H.S., R.J.D.) and Neuroradiology (K.S.), Montefiore Medical Center, 111 E 210th St, Bronx, NY 10467; Department of Radiology, Division of Emergency Radiology, Massachusetts General Hospital, Boston, Mass (L.L.A.); and Department of Dentistry and Maxillofacial Surgery, Brooklyn Hospital Center, Brooklyn, NY (H.D.). Received March 9, 2012; revision requested April 2 and received April 10; final version accepted June 18. For this journal-based CME activity, the authors, editor, and reviewers have no relationships to disclose. **Address correspondence to** M.H.S. (e-mail: *mscheinf@montefiore.org*).

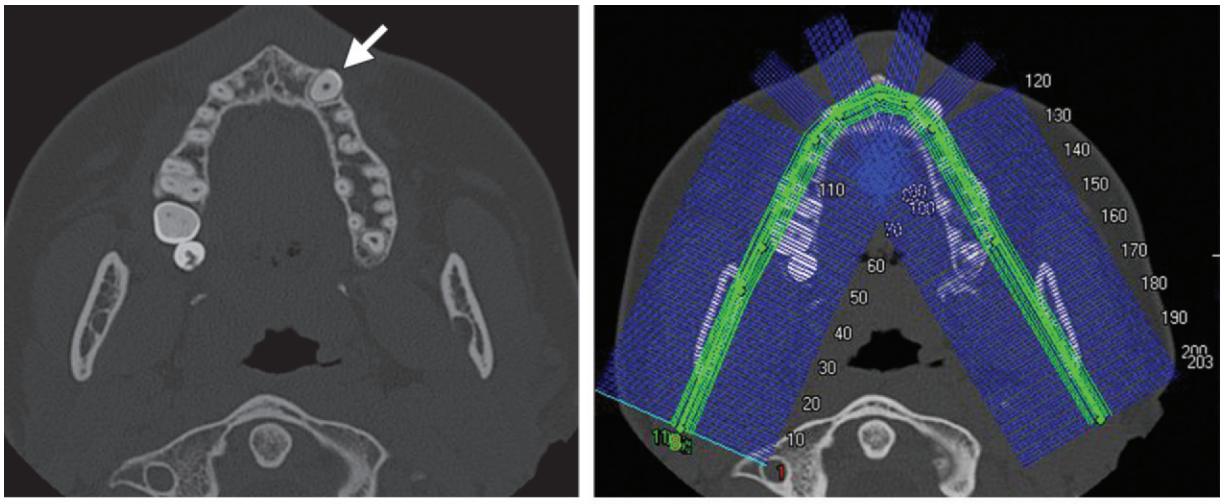

a. b.

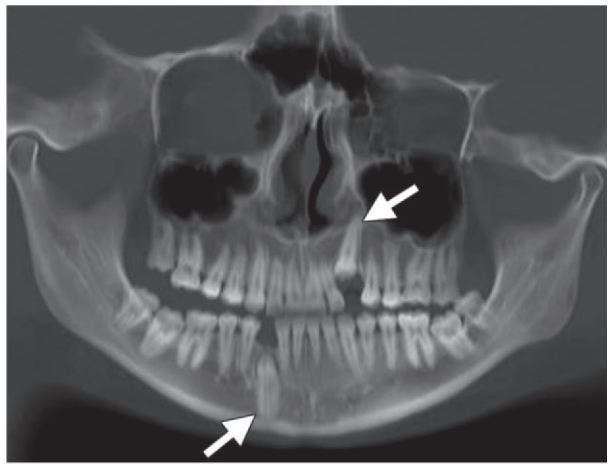

c.

Figure 1. Ex post facto reformation of facial CT images in a 19-year-old woman. **(a)** Axial CT image obtained at the level of the alveolar process of the maxilla shows a nonerupted left maxillary canine (arrow). **(b)** Dental panoramic curved planar reformatted CT image created to prepare for surgical and orthodontic eruption shows the contour lines of the jaw, which were added with software (TeraRecon, San Mateo, Calif). **(c)** Dental panoramic reconstructed CT image shows nonerupted left maxillary and right mandibular canines (arrows).

Introduction

In daily practice, although we do not intend to perform dental imaging, we frequently do. Whether imaging the brain, face, neck, sinuses, or cervical spine, images of the teeth and their surrounding bone and soft tissues are acquired. Often, an important pathologic condition that may be related to the patient's presenting symptoms is present but not recognized or mentioned by the interpreting radiologist (1). When interpreting multidetector computed tomographic (CT) images, the radiologist may provide added value by identifying definite or possible dental lesions and referring the patient to a dental specialist for clinical evaluation and dedicated radiography or cone-beam CT, as necessary (2). Dental and periodontal disease have also been linked to cardiovascular and systemic inflammatory disease, making identification important for early treatment (3–5,6).

Teaching Point

Both multidetector and cone-beam CT are able to generate three-dimensional (3D) image volumes of the oral cavity. Multidetector CT uses a fan beam, whereas cone-beam CT uses a cone-shaped beam, as its name implies (7). Multidetector CT has superior contrast resolution, greater signal-to-noise ratio, and intravenous contrast material capabilities, whereas cone-beam CT uses less radiation and has better spatial resolution and a lower cost (2,7–9). The advantages of cone-beam CT make it ideal for three-dimensional imaging of the teeth and oral bones, and multidetector CT (with or without intravenous contrast material) is more appropriate when images of soft tissues are also needed.

Images of head and neck structures are commonly obtained in multiple planes with different section thicknesses, each of which is best suited for depicting different aspects of odontogenic conditions. For example, carious lesions, which may be only 1 mm in diameter, are best seen on thin (0.5–0.6 mm)-section multidetector CT images. Periapical disease of the maxillary molars and its relationship to the sinuses are best depicted on coronal and sagittal images. Coronal images are

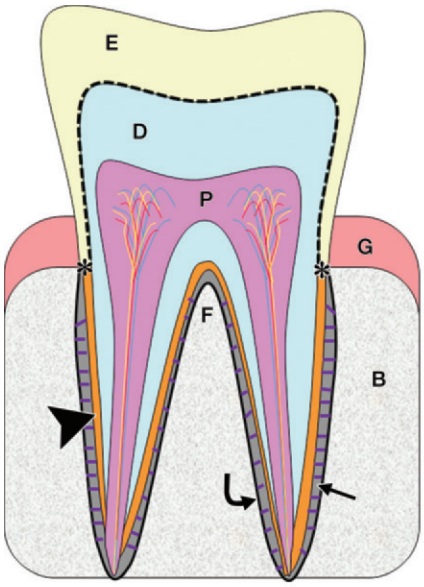

a.

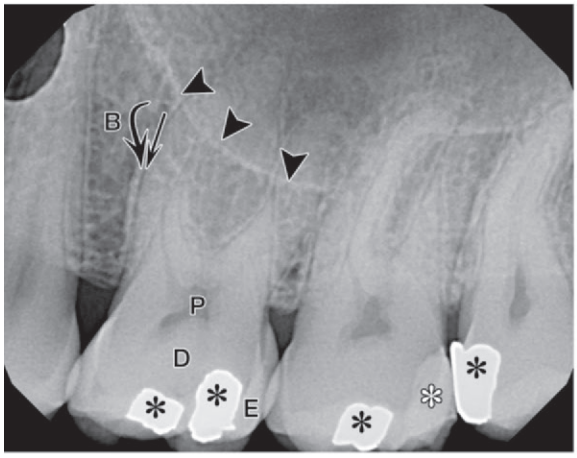

b.

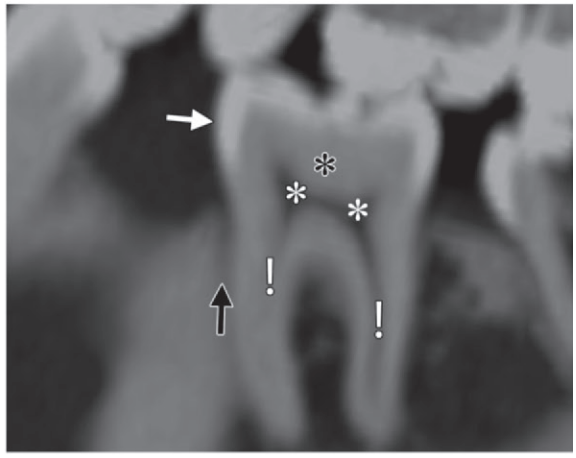

c.

Figure 2. Normal tooth anatomy. **(a)** Drawing shows normal tooth anatomy. Enamel *(E)* covers the crown, and a thin layer of cementum (arrowhead) covers the roots. Dentin *(D)*, a calcified matrix, lies between the enamel or cementum and the pulp chamber *(P)* or root canal. Cementum and dentin cannot be distinguished at imaging because they have similar mineralization. The pulp chamber and root canal contain neurovascular elements. Gingiva *(G)* covers the maxillary and mandibular alveolar processes *(B)*. In teeth with multiple roots, the space between the roots is called the furcation *(F)*. Lamina dura (curved arrow), a thin layer of dense bone, lines the socket. The periodontal ligament (straight arrow) lies between the lamina dura and cementum. ∗ = cementoenamel junction, dashed line = dentinoenamel junction. **(b)** Digital periapical radiograph of maxillary molars shows enamel *(E)*, dentin *(D)*, pulp chamber *(P)*, alveolar process *(B)*, lamina dura (curved arrow), and periodontal ligament space (straight arrow). Amalgam (black ∗) and composite fillings (white ∗) are also seen. Arrowheads = superimposed maxillary sinus wall. **(c)** Magnified sagittal oblique CT image of a mandibular molar shows the enamel (white arrow), dentin (black ∗), pulp chamber (white ∗), pulp or root canal (!), and periodontal ligament space (black arrow), which is radiolucent.

best for evaluating spread of odontogenic infections to the sublingual and submandibular spaces to determine their relationship to the mylohyoid muscle. Furthermore, with isotropic datasets (which may be routinely produced with CT scanners with 16 detector rows or more) and the increased capabilities of visualization software, oblique planar images, 3D surface-rendered images, and reconstructed dental panoramic images may be created post facto, when it is deemed necessary or useful for the patient's next step in care (Fig 1).

Imaging of jaw tumors has been well covered in the radiology literature (10–13). In this article, we discuss the multidetector CT appearance of dental inflammatory disease, which is more commonly encountered but has been less thoroughly covered (14).

Anatomy and Development

Teeth are composed of multiple components (Fig 2). The crown is covered by enamel, which is highly radiopaque. The root is enveloped by a thin layer of cementum. Dentin is located deep to the enamel and cementum and is isoattenuating relative to the cementum and hypoattenuating relative to the enamel. Dentin surrounds the root canal and pulp chamber, the most radiolucent tooth structures and which contain the neurovascular elements of the tooth (13). Teeth are held in their sockets by a periodontal ligament, which is seen as a thin radiolucent layer between the surface of the root and the lamina dura, the lining of the tooth socket. The lamina dura serves as

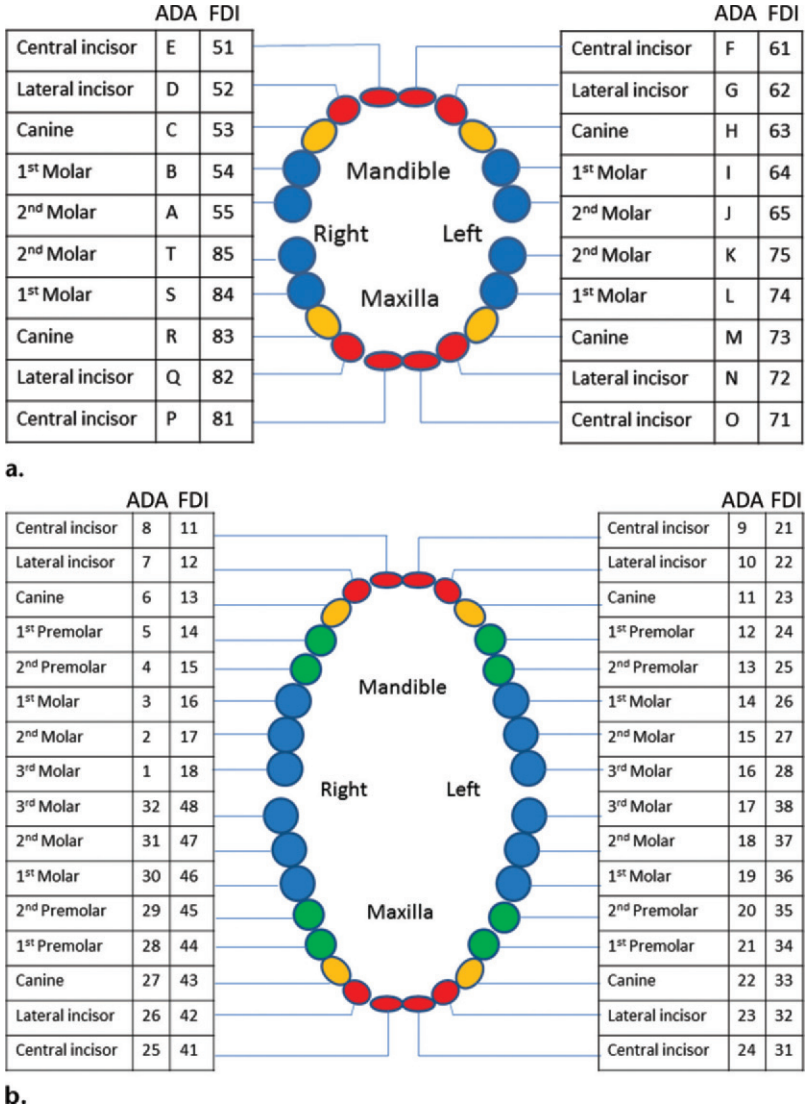

Figure 3. Tooth numbering nomenclature for primary and permanent teeth. **(a)** Illustration shows the universal numbering system (ADA), which uses letters A–T, and the FDI numbering system, which uses numbers 51–55, 61–65, 71–75, and 81–85, for primary teeth. Blue = molars, red = incisors, yellow = canines. **(b)** Illustration shows the universal numbering system (ADA), which uses numbers 1–32, and the FDI numbering system, which uses numbers 11–18, 21–28, 31–38, and 41–48, for permanent teeth. Blue = molars, green = premolars, red = incisors, yellow = canines.

the attachment site for the periodontal ligament; however, it may be discontinuous where the roots protrude into the maxillary sinus (15–17). Teeth are situated in the alveolar processes, which protrude from the maxilla and mandible. The height and thickness of these processes, as well as the body of the mandible, atrophy when teeth are absent (14). Each tooth and socket have an internal lingual surface and an external buccal surface.

There are two "sets" of dentition: primary (deciduous) and permanent. The primary teeth, of which there are 20, consist of a central incisor, lateral incisor, canine, first molar, and second molar in each quadrant, and there are usual age ranges for the development, eruption, and shedding of primary teeth (Fig 3) (18). The permanent teeth develop within the maxillary and mandibular bone from the occlusal surface toward the root apex and resorb the roots of the primary teeth as they migrate toward the oral cavity (19). Eruption continues until the tooth occludes with a tooth from the opposite jaw (18). The primary teeth are gradually replaced by 32 permanent teeth, which consist of a central incisor, lateral incisor, canine, two premolars, and three molars in each quadrant (Fig 3) (20). The American Dental Association (ADA) Universal Numbering System and the Federation Dentaire Internationale (FDI)–World Dental Federation notation are the two primary systems used to number teeth, with the ADA system more commonly used in the United States (Fig 3).

Following the principle "as low as reasonably achievable" (ALARA) and because of the continued campaigns to "Image Gently" in children and "Image Wisely" in adults, multidetector CT (with

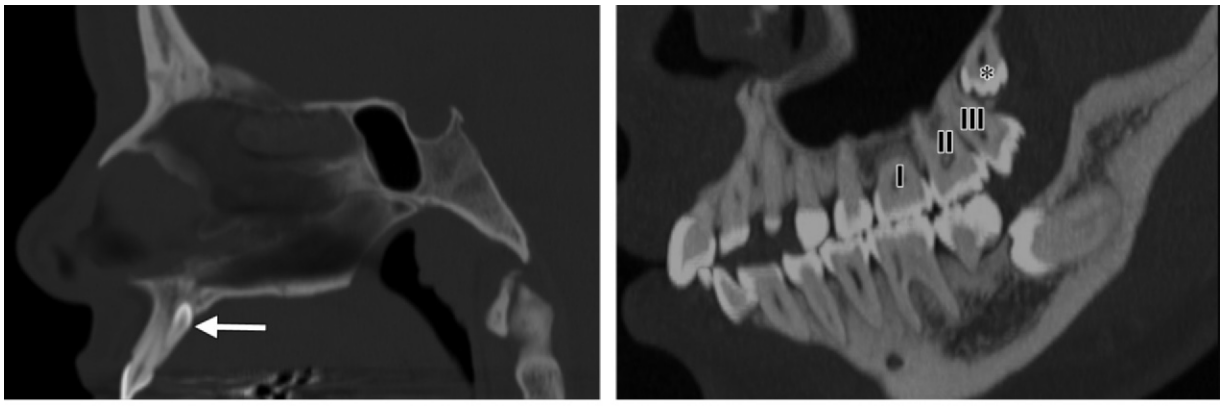

4. 5.

Figures 4, 5. **(4)** Mesiodens in a 34-year-old woman. Sagittal CT image shows a mesiodens (arrow) lingual to a maxillary incisor. The mesiodens appears peglike, with its crown facing superiorly, a common finding of this condition. **(5)** Supernumerary molar (distodens) in a 35-year old-woman. Sagittal oblique CT image shows an impacted supernumerary maxillary molar (*). *I, II, III* = normal three maxillary molars.

its relatively high radiation dose) is generally not the first-line modality used to evaluate anomalous development. Still, abnormal development, such as hyperdontia (more than 32 teeth) and hypodontia (fewer than 32 teeth), may be incidentally detected (21–24). Patients with supernumerary teeth may be asymptomatic. Supernumerary teeth may also damage or cause crowding of normal teeth or cause normal teeth to abnormally erupt or not erupt at all. Hyperdontia may be sporadic or associated with conditions such as Gardner syndrome and cleidocranial dysplasia (25). At imaging, hyperdontia may be recognized by the presence of more than 32 teeth or extra teeth outside the normal row. The frequency of hyperdontia varies among populations, with a recent study from the United States reporting that 44% of supernumerary teeth occur in the molar region, 33% in the premolar region, and 23% in the incisor region (23,25,26). A supernumerary tooth in the maxillary midline, adjacent to the incisors, is called a mesiodens, and a supernumerary molar posterior to the third molar is called a distodens (25) (Figs 4, 5). In many cases, the distodens may be impacted and cause dental infection and inflammation (27). Supernumerary teeth may be differentiated from odontomas, hamartomas of odontogenic origin that contain dentin, enamel, and cementum and the most common odontogenic tumor. Odontomas demonstrate varying degrees of disorganization, with a compound odontoma appearing more toothlike or as multiple small teeth and a complex odontoma appearing as a disorganized mass of tissue (28).

Hypodontia is less evident because lost (due to extraction, decay, or periodontal disease) and developmentally absent teeth may be difficult to distinguish. An impacted tooth is unable to fully erupt into the oral cavity, a result of obstruction by another tooth, and is well evaluated at CT; the third molars ("wisdom teeth") are frequently impacted (29). An impacted tooth may be a source of recurrent odontogenic pain, infection, and inflammation. Unerupted or impacted anterior teeth may also be identified at imaging and may require orthodontic or surgical treatment (Fig 1) (30).

Common Dental Restorations and Procedures

Dental restorations are commonly seen at CT. Restorations that contain a large amount of metal, such as dental implants and bridges, may cause substantial surrounding streak artifact and degrade image quality. Furthermore, beam hardening artifact from metallic fillings may cause an area of low attenuation at the interface between the filling and the tooth, giving the appearance of a recurrent carious lesion (31). Orthodontic appliances with a large metallic component may also cause severe streak artifact; however, hardware that contains less metal may be well seen at imaging.

Dental Amalgam

Dental amalgam, the material that is traditionally used to fill carious lesions, is composed of an alloy of mercury, silver, tin, copper, and, sometimes, zinc (32). Because of their metallic composition, these fillings may be surrounded by streak artifact. Resin composite and glass ionomer materials are also common filling and restorative agents. Resin composite material is composed of polymer resin (commonly bisphenol A dimethacrylate or

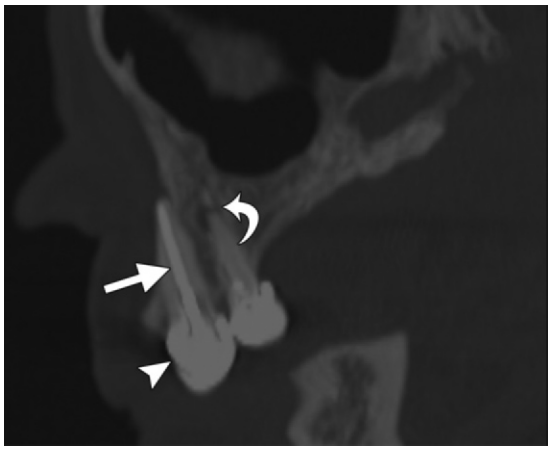

Figure 6. Root canal therapy in a 58-year-old woman. Sagittal CT image shows the appearance of root canal therapy, in which the pulp canal is filled with gutta-percha (straight arrow), and the tooth is restored with a metallic crown (arrowhead). An area of radiolucency (curved arrow) indicative of apical periodontitis is also seen at the root apex of the adjacent first premolar.

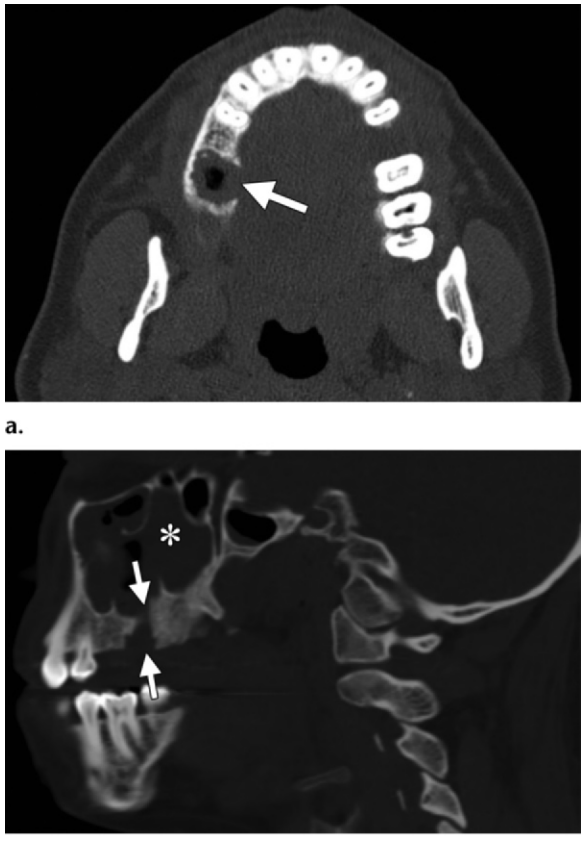

a.

b.

Figure 7. Oroantral fistula. Axial **(a)** and sagittal **(b)** CT images show an absence of bone separating the first maxillary molar tooth socket from the maxillary sinus (arrows in **b**) and a loss of continuity of the palatal cortical plate (arrow in **a**). Fluid and mucosal thickening are also seen within the maxillary sinus (∗ in **b**), a characteristic finding of oroantral fistula.

urethane dimethacrylate), binding agents, barium or strontium to make it radiopaque, initiators to trigger the curing process, and other fillers (32). Resin composite is less radiopaque than amalgam and does not create prominent streak artifact (Fig 2). Glass ionomer materials have different compositions but are usually a composite of fluoroaluminosilicate and polyalkenoic acid (or its derivative), as well as metallic agents to render the material radiopaque (33). Aside from the cosmetic desirability of these nonamalgam materials, from an imaging standpoint, their use has been advocated in patients with head and neck cancer who require regular follow-up at CT (34).

Root Canal Therapy

Root canal therapy is the endodontic technique of treating dead or infected pulp. After gaining access to the pulp chamber, usually by way of the crown of the tooth, the chamber and canals are cleaned and disinfected, and the empty canals are filled, most commonly with a compound composed of zinc oxide and gutta-percha, a natural nontoxic latex with antimicrobial properties (35). Other substances such as synthetic rubber, carbon, and metals may also be used. After the canal is filled, a post and crown may be added to reinforce the devitalized tooth (Fig 6).

Extraction

The socket of a recently extracted tooth first fills with radiolucent granulation and gingival tissue. If there are no complications, the extraction site remodels over 6–8 weeks and becomes radiographically indistinct by 8 months (36). When a maxillary tooth is extracted, a connection between the tooth socket and the maxillary sinus may form. If its diameter is less than 2 mm, it usually closes by itself (17). A larger connection may lead to formation of a tract lined with epithelial cells, called an oroantral fistula, which may require closure with a surgical flap (32). Oroantral fistula is usually clinically diagnosed on the basis of bubbles emanating from the tooth socket when the nose is blown with the nostrils closed. At imaging, oroantral fistula may appear as an interruption of the cortical floor of the sinus overlying the extraction socket, with fluid and mucosal thickening in the maxillary sinus (Fig 7) (37). After a tooth is extracted, the opposing tooth on the opposite jaw may gradually hypererupt (Fig 8) (38). Rarely, in the immediate postprocedure period, subcutaneous emphysema, pneumomediastinum, or pneumothorax may result from the pressurized air in air turbine dental drills (Fig 9) (39,40).

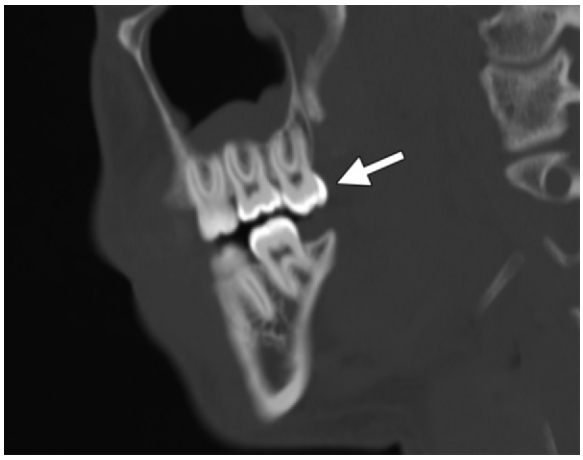

Figure 8. Hypereruption in a 21-year-old man. Sagittal CT image shows hypereruption of the third maxillary molar (arrow), which occurred after the third mandibular molar was extracted.

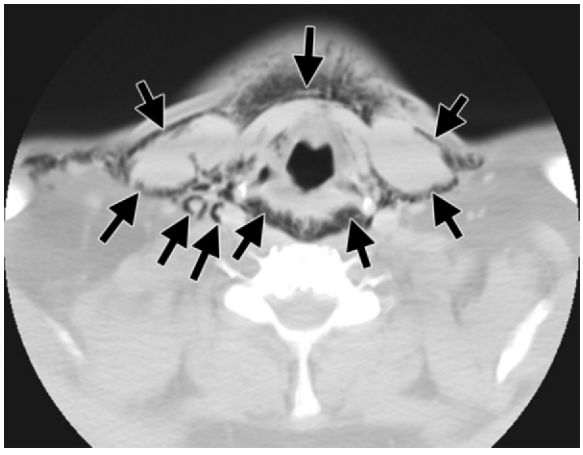

Figure 9. Subcutaneous emphysema in a 58-year-old man who underwent extraction of a maxillary molar with a compressed air–driven drill. CT image of the neck shows extensive subcutaneous emphysema. Air (arrows) is seen outlining the tissue planes, including the right carotid artery and internal jugular vein.

Tooth Trauma

Tooth fractures are difficult to detect. Because of its relatively low radiation dose, low cost, and high spatial resolution, cone-beam CT is well suited to cases in which a fracture is the sole clinical question. However, patients who undergo multidetector CT for other reasons (eg, evaluation of facial trauma) should also be evaluated for tooth fractures. Nondisplaced tooth fractures may be seen as a linear area of low attenuation traversing the tooth (Fig 10). Importantly, vertical root fractures are not well seen on dental radiographs but may be definitively diagnosed at multidetector and cone-beam CT (41). When the fractured fragment is displaced, surface-rendered images offer the best perspective for visualizing the irregular edges of the broken tooth. Although dental fractures are usually evident at clinical examination, they may be missed in the context of severe facial trauma with concomitant injuries. Tooth fragments or entire teeth may be aspirated (usually due to facial trauma or intubation) and are seen at subsequent chest or abdominal radiography. Tooth avulsion or luxation (loosening), which may also be associated with socket fractures, is well seen at CT as widening of the periodontal ligament space, a condition that most commonly affects the central incisors in children who are between 7 and 14 years old (Fig 11) (42). Early diagnosis of tooth avulsion while the periodontal ligament cells are still viable allows for early tooth reimplantation and better outcomes (42).

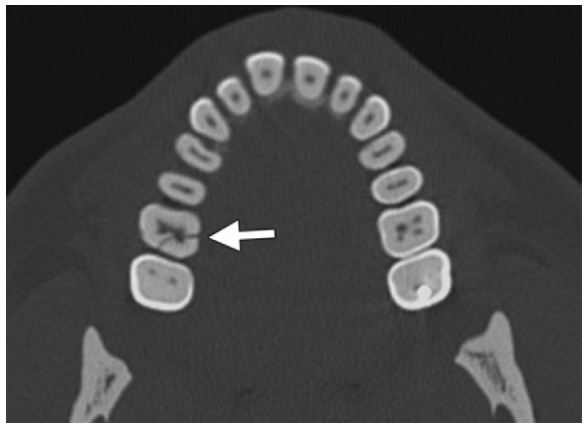

Figure 10. Tooth fracture in a 55-year-old man. Axial CT image of the maxilla shows a thin curvilinear area of low attenuation, a finding indicative of a vertical tooth fracture (arrow).

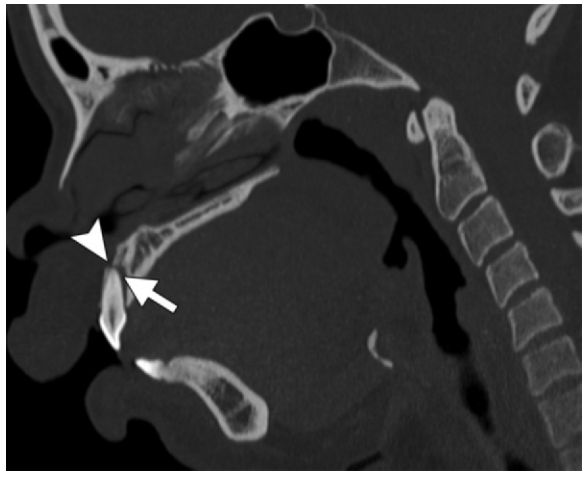

Figure 11. Tooth avulsion in a 21-year-old woman. Sagittal CT image shows widening of the periodontal ligament space (arrow) and fracture of the buccal surface of the alveolar process (arrowhead).

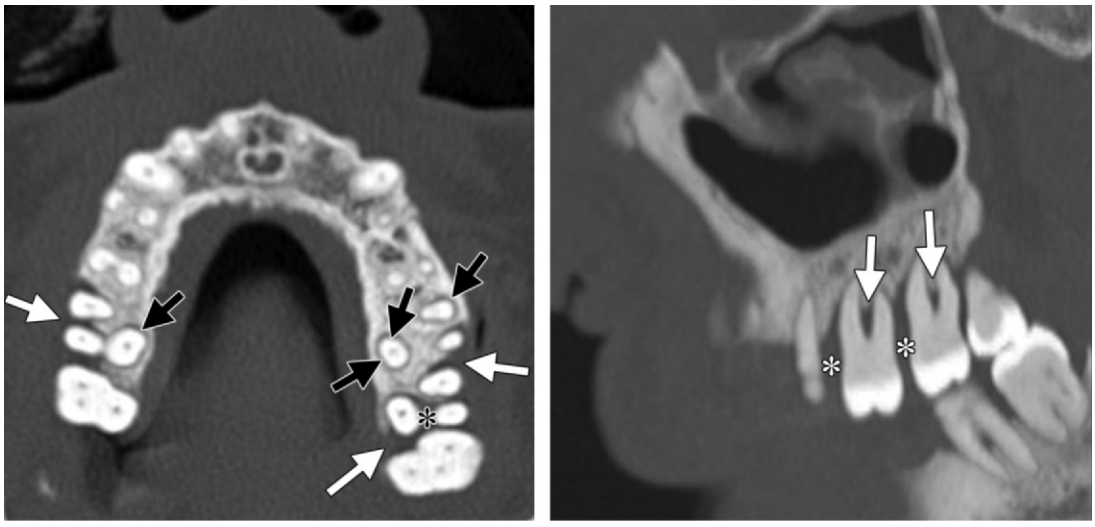

a. b.

Figure 12. Periodontal disease in a 52-year-old man. **(a)** Axial CT image shows marked bone loss (white arrows) around the molar roots and widening of the periodontal ligament space, which is seen as a ring of low attenuation (black arrows) surrounding the molar roots. Bone loss is also seen at a molar furcation (*). **(b)** Sagittal oblique CT image shows bone loss between the teeth (*) and at furcations (arrows). **(c)** Three-dimensional surface-rendered CT image shows marked bone loss, with partial uncovering of the roots in multiple premolars and molars (*).

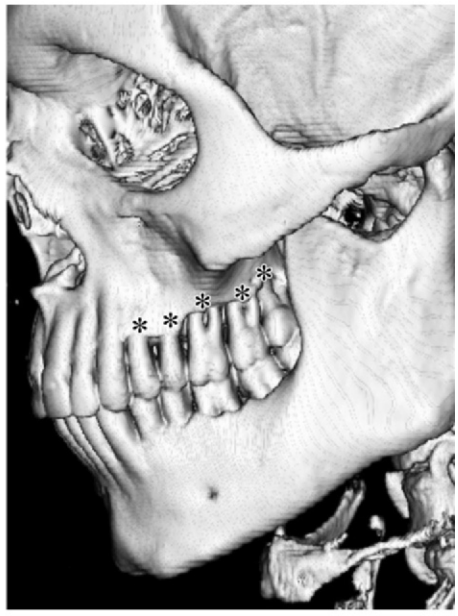

c.

Periodontal Disease

Periodontal disease is the most common cause of tooth loss worldwide (43). When dental care is inadequate, bacteria-harboring plaque accumulates at the tooth-gingival (gum) interface, leading to inflammation of the gingiva, a condition known as gingivitis. Plaque infection may extend under the gingiva, creating a periodontal pocket. In marginal periodontitis, the infection spreads along the periodontal ligament toward the tooth apex, destroying the periodontal ligament and resorbing bone between teeth and at root furcations (14). Ultimately, general tooth loosening and root uncovering result.

At imaging, periodontal disease with destruction of periodontal ligaments appears as widening of the normal, thin periodontal ligament space (Fig 12). Widening of this space is nonspecific and may also occur with orthodontic treatment, apical periodontitis, traumatic loosening, bruxism, systemic sclerosis, and, when limited to one or two teeth, osteosarcoma (Fig 11) (44,45). In periodontitis, bone loss occurs between teeth and at the furcations between roots, thereby uncovering the tooth roots, which are normally covered by the bone of the alveolar processes (Fig 12).

Teaching Point

Pericoronitis is a special category of gingivitis that occurs when the gingiva overlying the crown of a partially erupted tooth, which is frequently impacted, becomes inflamed (Fig 13) (46). The third mandibular molar is most commonly affected. Spread of infection from the involved tooth, usually through the thinner lingual plate of the alveolar process, may lead to deep neck infection and involve the masticator, submandibular, parapharyngeal or, least commonly, sublingual space (47). Definitive treatment usually involves extraction of the involved tooth (48).

Carious Lesions

Despite their decreased incidence after the introduction of fluoride, carious lesions are still very common among the general population and, consequently, are frequently seen at CT (49). Carious

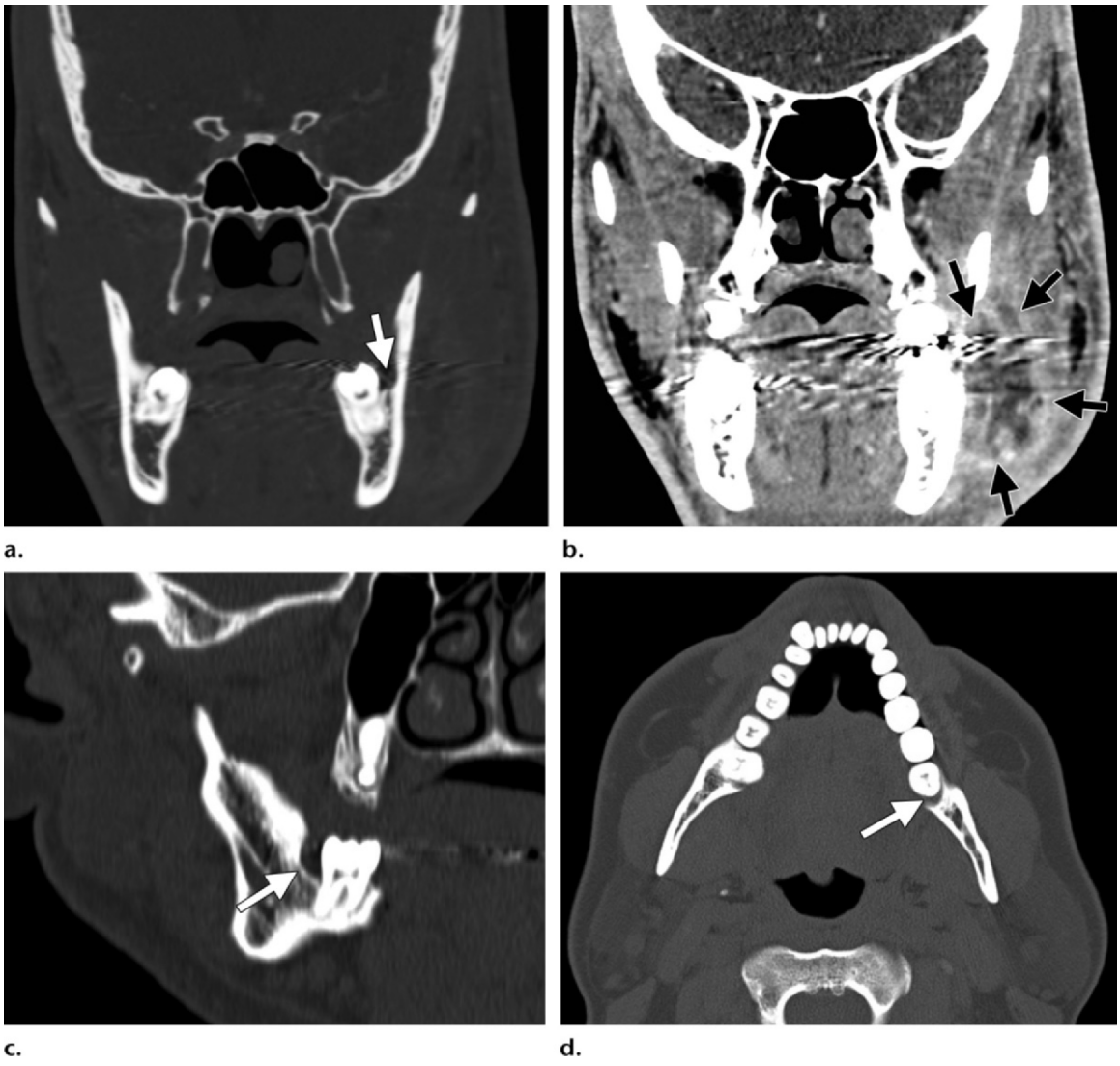

Figure 13. Pericoronitis in two patients. **(a)** Coronal CT image obtained with bone window settings in a 24-year-old man shows an impacted left third mandibular molar and expansion of the buccal coronal follicular space (arrow). **(b)** Coronal CT image obtained with soft-tissue window settings in the same patient shows an adjacent abscess in the masticator space (arrows). Streak artifact from dental amalgam extends through the abscess. **(c, d)** Sagittal **(c)** and axial **(d)** CT images obtained with bone window settings in a 31-year-old man show distocoronal chronic pericoronitis (arrow) involving the bone posterior to the mandibular third molar. A widened distocoronal follicular space and adjacent bone sclerosis are also seen, common changes, especially in young adults, that are most often accompanied by a partial soft-tissue covering (operculum) of the third molar that becomes intermittently inflamed, traps food and debris, and leads to the gradual destruction of and adjacent sclerosis in the bone adjacent to the crown of the tooth. (Figure 13c and 13d courtesy of Alan G. Lurie, DDS, PhD, University of Connecticut School of Dental Medicine, Farmington, Conn.)

lesions have also been seen with a clinical MR imaging system, but this technique is still mostly limited to the research realm (50). The detection of carious lesions by the radiologist should alert the care team to recommend a follow-up dental examination.

Carious lesions are foci of enamel and dentin demineralization caused by acid produced by bacterial fermentation of carbohydrates (32). Carious lesions may take years to penetrate through the enamel. Remineralization may cause them to regress, especially in the presence of fluoride (32). Once decay reaches the dentinoenamel junction, it spreads more easily and rapidly through the dentin, and the infection undermines the overlying enamel (32). Occlusal caries are on the chewing surface of the tooth, whereas approximal caries are between teeth. Saliva reduces the incidence of carious lesions, likely by neutralizing acid produced by cariogenic *Streptococcus mutans* and assisting in remineralization (51). Patients with xerostomia

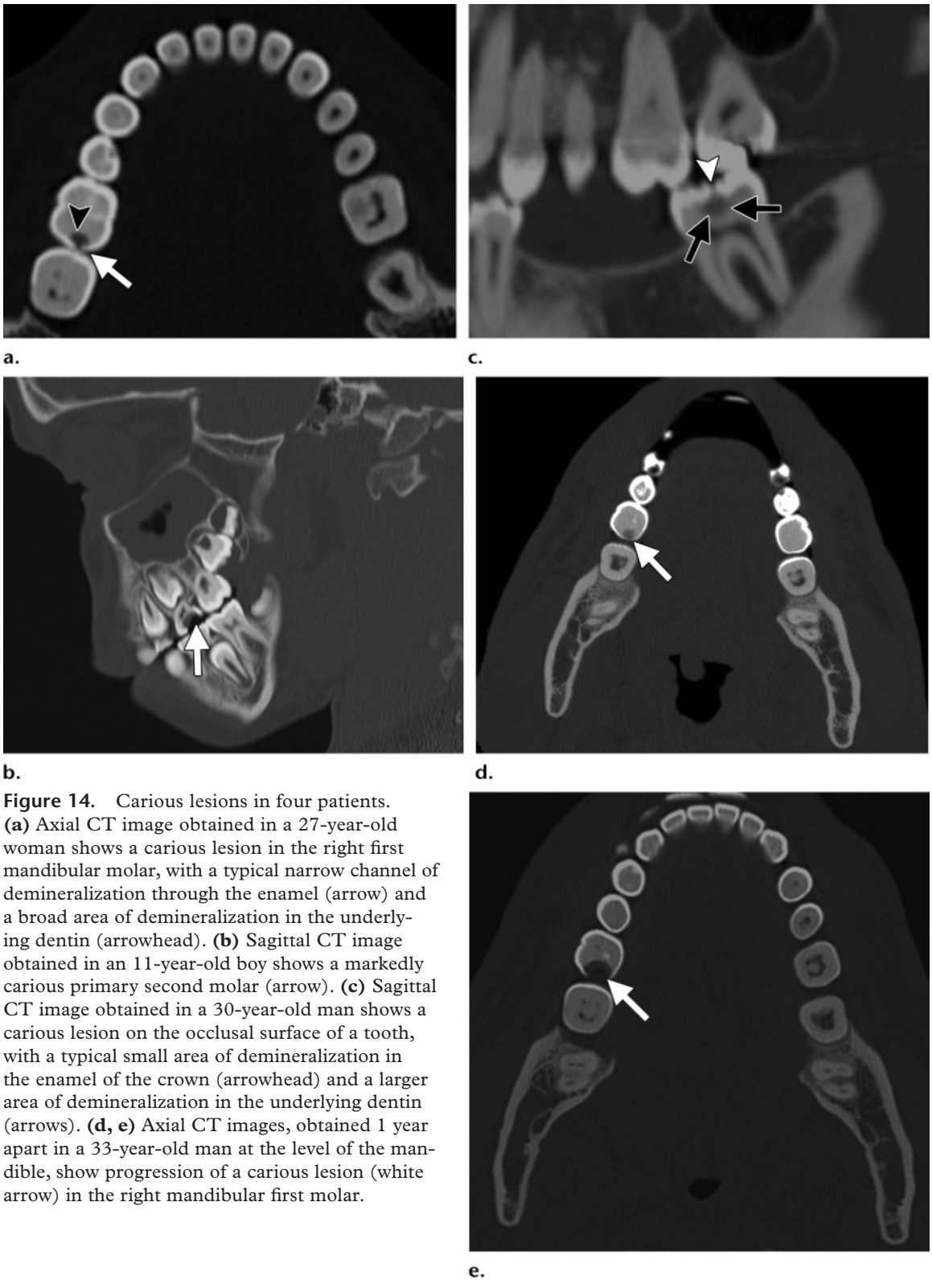

Figure 14. Carious lesions in four patients. **(a)** Axial CT image obtained in a 27-year-old woman shows a carious lesion in the right first mandibular molar, with a typical narrow channel of demineralization through the enamel (arrow) and a broad area of demineralization in the underlying dentin (arrowhead). **(b)** Sagittal CT image obtained in an 11-year-old boy shows a markedly carious primary second molar (arrow). **(c)** Sagittal CT image obtained in a 30-year-old man shows a carious lesion on the occlusal surface of a tooth, with a typical small area of demineralization in the enamel of the crown (arrowhead) and a larger area of demineralization in the underlying dentin (arrows). **(d, e)** Axial CT images, obtained 1 year apart in a 33-year-old man at the level of the mandible, show progression of a carious lesion (white arrow) in the right mandibular first molar.

(such as occurs in Sjögren disease), who are taking psychoactive medications, or who are undergoing radiation therapy for head and neck cancer may develop many carious lesions because of altered oral flora and reduced acid-neutralizing saliva (52,53). Such lesions are typically cervical, which means they are located at the gingival margin at the cementoenamel junction (54).

At CT, carious lesions appear as focal areas of enamel and dentin loss that extend from the surface of the tooth (Fig 14) (2). Early carious lesions commonly have a mushroom shape, with the "stalk" representing a narrow channel through the enamel and the "head" representing a larger area of dentin demineralization undermining the enamel. Lesions in the anterior teeth and advanced lesions in the posterior teeth are more ovoid. Caries may be single or multiple, and when severe, they may be associated with periapical and periodontal disease. Severe carious involvement of deciduous teeth may progress to apical or furcational periodontitis, which may lead to malformation or death of the underlying developing permanent tooth and, ultimately, noneruption. Carious lesions may recur after a tooth is filled or crowned and appear as a new area of low attenuation deep to the filling or crown. However, these lesions generally require intraoral radiography for depiction. As was mentioned earlier, multidetector CT has inferior spatial resolution compared with that of cone-beam CT (which has isotropic spatial resolution of at least 0.15 mm) and, when necessary, sagittal cone-beam CT images may be useful, particularly in evaluating the occlusal surfaces of teeth (7).

Teaching Point

Periapical Disease

Teaching Point

Apical periodontitis refers to a spectrum of diseases that occur around the tooth apex, including periapical granuloma, periapical abscess, and periapical (radicular) cyst (35,55). Infection of the pulp, which usually results from carious lesions that have reached the pulp chamber, increases pressure within the chamber and activates pain fibers within the pulp, causing extreme pain. Persistent high pressure within the pulp chamber leads to pulp death and devitalizes the tooth. Infectious or inflammatory material (even in the absence of infection) in the canal ultimately decompresses into the periapical bone, causing an acute phase of bone resorption. A subacute periapical granuloma may occur at a site of granulation tissue formation where there is a balance between the formation and neutralization of infectious and inflammatory material (35). A radicular cyst, an expansile epithelium-lined cavity that contains fluid or semisolid material, may ultimately form within the maxilla or mandible (35). Rarely, if the offending tooth is extracted and the periapical lesion is not curetted, the remaining cyst is referred to as a residual cyst (35).

As was described earlier, leukocytes are generally effective in restricting bacteria to the root canal and periapical region (in the form of a granuloma or cyst). When an organized cavity is not formed or the balance between the formation and neutralization of infectious and inflammatory material is interrupted (eg, after root canal therapy), a painful periapical abscess may form and remain within the bone as an intraalveolar abscess. Acute osteomyelitis may also develop, appearing as an area of permeative "lucency" within the bone; chronic osteomyelitis leads to sclerosis of the surrounding bone. Infection may also break through the lingual or buccal cortices of the alveolar process and drain into the adjacent soft tissues or maxillary sinus (35). In teeth with more than one root, the cortical surface that is penetrated depends on which cortex is adjacent to the involved root.

Treatment of periapical disease consists of root canal therapy, surgery, tooth extraction, or a combination of these methods (10,32,56). When extraction is performed, osseointegrated implants are the treatment of choice to restore a functional and cosmetic tooth (57). For treatment of a small periapical lesion associated with a nonvital tooth, root canal therapy is often adequate. For larger lesions, a surgical procedure is usually required in addition to root canal therapy. In such cases, a typical tooth-saving approach involves creation of a mucoperiosteal flap over the apex of the tooth, removal of the overlying bone, and enucleation of the debris within the lesion. The apex of the tooth is then excised and the root canal filled retrograde, most commonly with amalgam. As healing progresses, the periapical lucency may fill with bone, scar tissue, or a combination of both.

The three forms of periapical disease (granuloma, abscess, and cyst) have similar, but not identical, imaging appearances. In all three, an

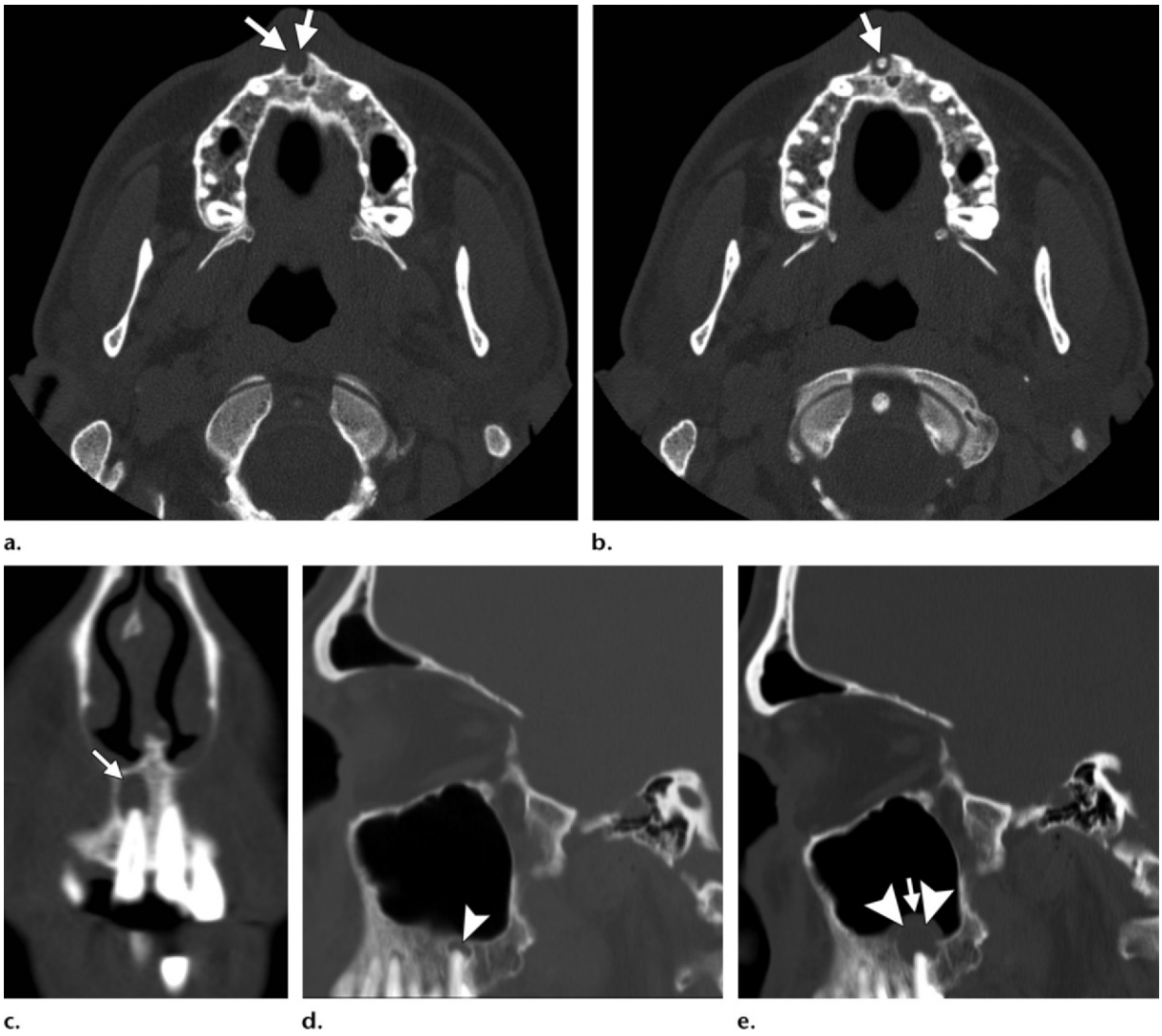

Figure 15. Periapical lucency in two patients. **(a)** Axial CT image obtained in a 26-year-old man at the level of the maxilla shows a periapical lucency at the right central incisor (arrows). **(b)** Axial CT image obtained more inferiorly shows the lesion, which demonstrates a target or bulls-eye appearance, with a central area of high attenuation that represents the root apex (arrow). **(c)** Coronal CT image shows the relationship of the periapical lucency (arrow) with the tooth apex. **(d)** Sagittal CT image obtained in a 50-year-old man shows a periapical granuloma (arrowhead) at a maxillary molar. **(e)** Sagittal CT image obtained in the same patient 3 years later shows the granuloma (arrowheads), with marked thinning of the surrounding bone and superior displacement and reactive mucosal thickening of the floor of the maxillary sinus (arrow).

area of lucency is seen around the tooth apex. Keratocystic odontogenic tumors may have a similar appearance as periapical lesions, adding further diagnostic uncertainty (58). In the literature, there are conflicting reports regarding whether the presence of a sclerotic rim at radiography may differentiate a periapical cyst from a periapical granuloma (10,59–61). With CT, some studies report that they may be differentiated on the basis of attenuation, with cysts having low attenuation values and granulomas having higher attenuation values (62,63). However, a small lesion size, coexistent periapical lesions, and persistent infection or inflammation may cause attenuation values to vary, making this approach unreliable. Differentiating periapical cysts and granulomas may not be necessary because patients with both types undergo treatment when the lesions reach a certain size: Those with cysts are treated to prevent continued expansion, and those with granulomas are treated to remove the smoldering inflammatory

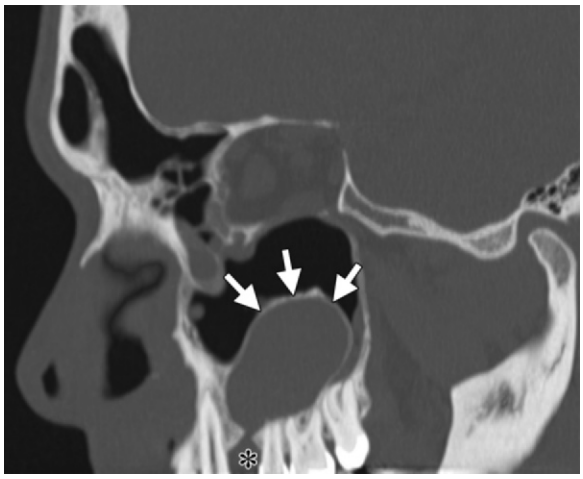

Figure 16. Residual cyst in a 33-year-old man. Sagittal CT image obtained centered over the maxilla shows a large residual cyst (arrows) that originates at the site of an extracted first premolar (*) and balloons into the maxillary sinus.

process. Periapical abscess may not demonstrate an area of periapical lucency within the first 10 days because sufficient bone resorption has not yet occurred. Still, clinical symptoms such as severe pain and swelling are invariably present, and imaging findings of a deep carious lesion and widening of the periodontal ligament space may be seen (46). After treatment, the periapical lucency usually begins to fill with bone over 2–4 months, with some healing present within 1 year in 89% of lesions (15,64).

The relationship of a periapical lesion with an anterior tooth and adjacent bone is best depicted on coronal images, and that with a posterior tooth and adjacent bone is best seen on sagittal images (Fig 15). On axial images, lesions are seen as a focus of lucency distal to the root. At the level of the root, a central focus of high attenuation represents the root, and a surrounding area of lucency represents resorbed bone (Fig 15). Adjacent areas of increased bone density may extend as much as 22 mm into the surrounding bone, a finding that represents sclerosing osteitis, a reactive proliferation of sclerotic bone (65). Residual cysts have the same appearance as periapical cysts, with absence of an affected tooth (Fig 16) (66). From an imaging standpoint, the differential diagnosis for a periapical lucency includes periapical cemento-osseous dysplasia, hyperparathyroidism, Langerhans cell histiocytosis, keratocystic odontogenic tumor, leukemia, and lymphoma (10,67). The presence of coexisting lesions, such as deep carious disease, favors apical periodontitis; findings from physical examination, such as pulp vitality testing, and clinical history help correctly diagnose the lesion.

Odontogenic Sinusitis

Studies have reported that 5%–38% of cases of maxillary sinus mucosal disease are caused by apical periodontitis and periodontal disease (16,17,68). What were once dismissed as polyps and retention cysts may now be seen as odontogenic mucosal disease at CT (14). Differentiating between sinusitis caused by obstructed drainage pathways and odontogenic disease is important to direct patients to the most appropriate treatment. Failure to identify the source of odontogenic disease leads to recurrent sinusitis after cessation of antibiotic therapy (1). The organisms that are found in patients with odontogenic sinusitis are different than those that are isolated in patients with nonodontogenic sinusitis (69). In one study, patients with maxillary sinus mucosal thickening who underwent treatment for periodontal disease demonstrated subsequent regression of sinus mucosal disease (70).

Symptoms of odontogenic sinusitis include purulent nasal discharge, cheek and facial pain, and facial pressure (71). Initially, these symptoms may be subtle because of decompression of the infection by way of the patent ostiomeatal unit and because sinus pressure does not build up (as it does in sinusitis caused by obstruction of the ostiomeatal unit). Treatment typically involves treating the causative periodontal disease, extracting or performing root canal therapy in the involved tooth or teeth (if apical periodontitis is present), performing sinus drainage, and administering antibiotic therapy (72). Conversely, it is important to recognize that sinus

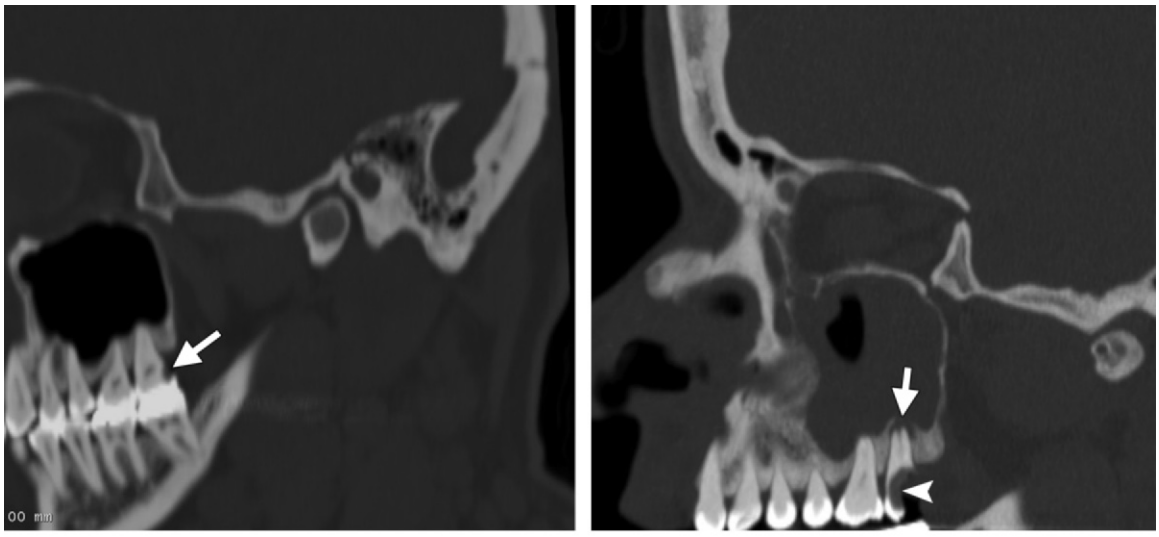

a. b.

Figure 17. Progression of a carious tooth to odontogenic sinusitis over a period of 3 years and 2 months. **(a)** Sagittal CT image shows a carious lesion (arrow) in the second maxillary molar. **(b)** Sagittal CT image obtained 3 years and 2 months later shows marked progression of the carious lesion (arrowhead) and a new periapical lucency (arrow), a finding consistent with apical periodontitis. Gross dehiscence of the periapical bone (arrow) is also seen, with near total opacification of the maxillary sinus, a finding indicative of odontogenic sinusitis.

floor mucosal inflammation may manifest with toothache and masquerade as a primary dental problem (73). However, symptoms of sinus floor mucosal inflammation usually affect multiple teeth (17).

In the past, the close relationship between the roots of the maxillary teeth and the maxillary sinuses was not always appreciated because of the routine use of axial imaging and nonisotropic datasets (16). Now, this relationship is apparent due to the ready availability of coronal and sagittal reconstructions with multidetector and cone-beam CT (7). The roots of the maxillary teeth may protrude into the maxillary sinus, with only a thin layer of mucosa—with or without bone—separating the tooth from the sinus. Infection or inflammation may penetrate the mucosal layer, which is thinnest over the second maxillary molar (68). Because of its three-dimensional, submillimeter capabilities, CT may be thought of as the new reference standard for depicting odontogenic sinus disease (71).

Teaching Point

The relationship between the teeth and the maxillary sinus is best seen on sagittal and coronal images (Fig 17) (16). Sinus mucosal thickening associated with focal ballooning or dehiscence of the floor of the maxillary sinus above a carious tooth is highly suspicious for an odontogenic source of infection. In addition, an unerupted tooth in the maxillary sinus may be a nidus of sinusitis (Fig 18) (74).

Deep Neck Infections

Severe periapical, periodontal, and pericoronal disease may extend into the deep tissues of the head and neck. Patterns of spread have been studied, with varying conclusions. The parapharyngeal, submandibular, anterior visceral, masticator, and sublingual spaces are reported to be commonly involved (46,75–77). Infection may even spread far from the teeth and cause conditions such as orbital cellulitis and mediastinitis, and it may be seeded or forced into the adjacent soft tissues by dental procedures such as root canal and tooth extraction (78–80). Spread of infection may manifest with local symptoms, such as pain, swelling, and warmth, or systemic symptoms, such as fever, chills, and elevated blood and serum inflammatory markers (46).

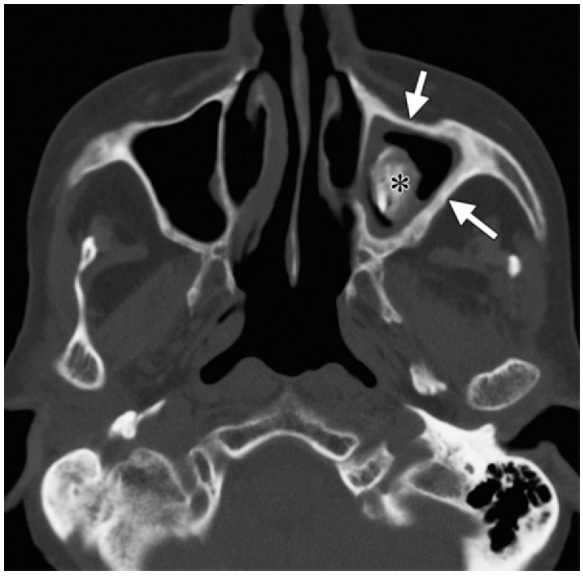

Figure 18. Sinusitis from an ectopic tooth in an 81-year-old woman. Axial CT image shows an ectopic tooth in the maxillary sinus (*), with associated mucosal thickening and asymmetric cortical thickening (arrows), findings consistent with chronic sinusitis.

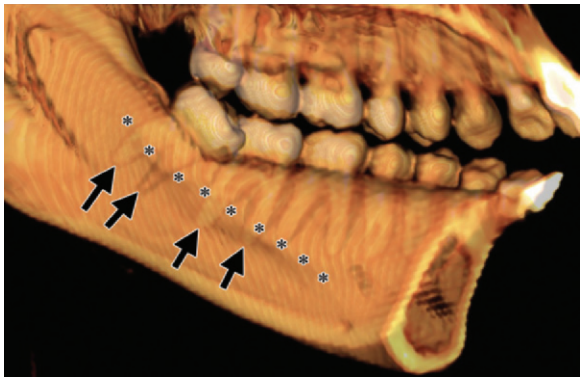

Figure 19. Relationship of the mandibular molar roots to the mylohyoid ridge. Sagittal surface-rendered CT image of the internal aspect of the mandible shows extension of the roots of the second and third mandibular molars (arrows) below the mylohyoid ridge (*), the attachment site of the mylohyoid muscle. (Transparency of the bone was adjusted to depict ghost images of the tooth roots through the cortex.)

Abscesses in the parapharyngeal, submandibular, anterior visceral, masticator, and sublingual spaces are best depicted at contrast-enhanced CT and appear as an irregular fluid collection

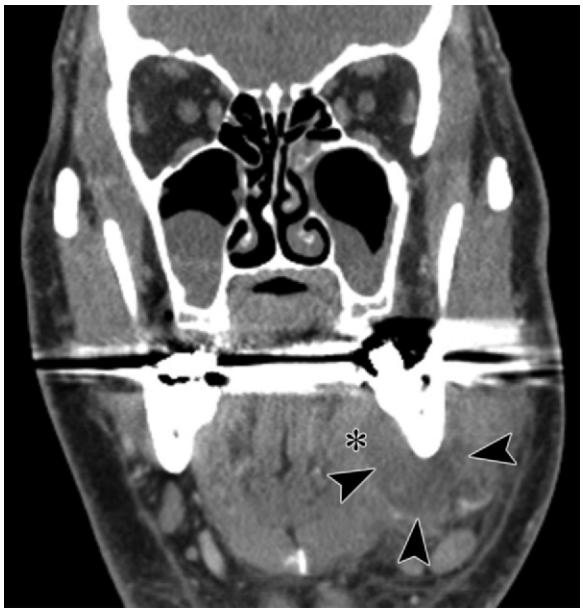

Figure 20. Odontogenic submandibular abscess. Coronal CT image shows a submandibular abscess (arrowheads) adjacent to the left mandibular second molar and medial bowing of the mylohyoid muscle (*).

with rim enhancement. Subtle odontogenic infection may be identified as stranding in the fat adjacent to the teeth and thickening of the overlying platysma muscle. Traditionally, initial spread of mandibular periapical disease to the sublingual or submandibular spaces has been linked to the location of the involved tooth roots relative to the attachment of the mylohyoid muscle (Fig 19). In general, periapical infection of the second and third mandibular molars spreads to the submandibular space first because the roots of these teeth terminate below the mylohyoid muscle. Periapical infection of the other mandibular teeth, whose roots terminate above the mylohyoid muscle, generally involves the sublingual space first (76). Regardless of the initial location of disease relative to the mylohyoid muscle, infection may spread between these spaces and around the posterior free margin of the mylohyoid muscle, as well as to other deep neck spaces (Fig 20) (81). Spread of infection into the deep neck spaces may also cause osteomyelitis of adjacent bone (Fig 21).

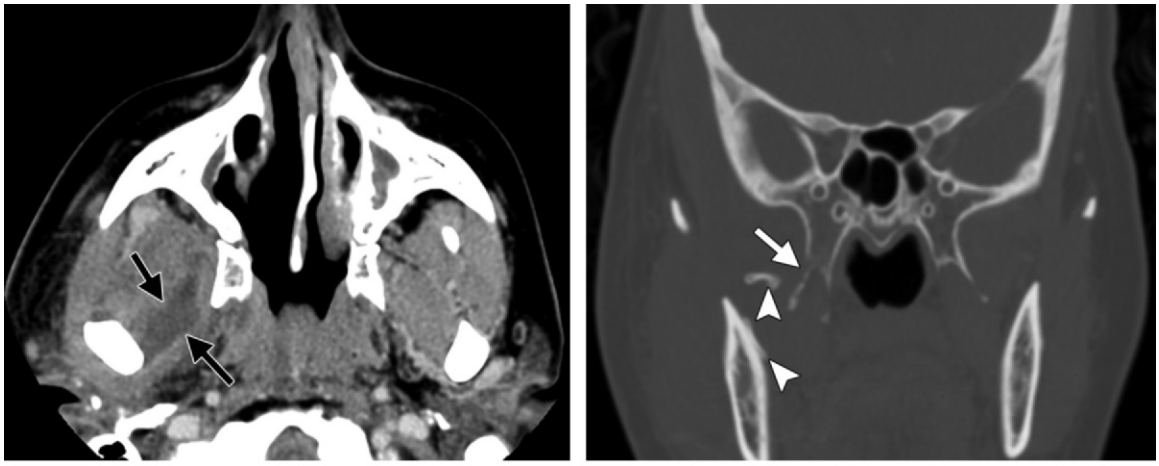

a. b.

Figure 21. Abscess and osteomyelitis in the masticator space. **(a)** Axial CT image shows an abscess (arrows) in the right masticator space that developed after extraction of the right maxillary third molar, which was carious. **(b)** CT image obtained 1 week later shows cortical bone loss within the pterygoid plates (arrow), a finding consistent with osteomyelitis. Two surgically placed drains (arrowheads) are also seen in the masticator space.

Extension of odontogenic cellulitis or abscess into the bilateral submandibular and sublingual spaces may lead to Ludwig angina, symptoms of which include fever, firm neck swelling and edema, and difficulty swallowing or speaking (Fig 22) (82). Patients with Ludwig angina are treated with antibiotic therapy, aggressive drainage, and surgical airway creation as needed (83).

Conclusions

The teeth and their support structures are commonly included on head and neck images. When normal variants or pathologic conditions are identified at CT, radiologists may provide additional assistance by identifying these conditions and including them in their report. The ability to recognize and describe dental conditions, such as caries, periodontal disease, and periapical lesions, allows timely referral to a dental specialist and early definitive treatment to prevent continued pain, morbidity, and tooth loss.

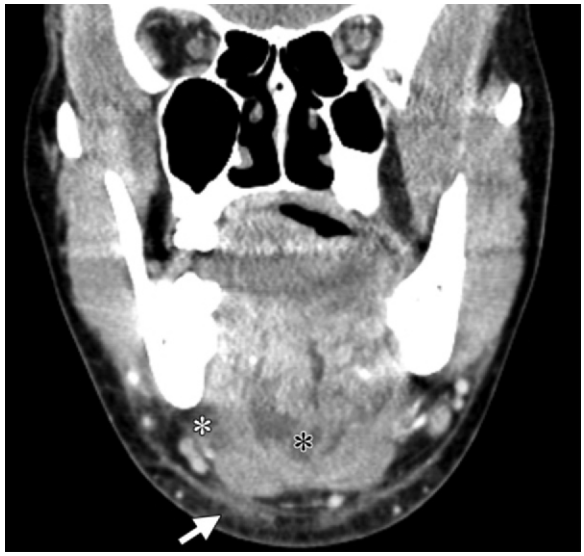

Figure 22. Ludwig angina. Coronal contrast-enhanced CT image shows an abscess in the right submandibular space (white *) and bilateral sublingual spaces (black *), a result of an infection in the right mandibular second and third molars. Subcutaneous edema and thickening of the platysma muscle are also seen (arrow). The patient was hospitalized for 5 weeks with multiple complications but ultimately recovered.

References

1. Longhini AB, Ferguson BJ. Clinical aspects of odontogenic maxillary sinusitis: a case series. Int Forum Allergy Rhinol 2011;1(5):409–415.
2. Tyndall DA, Rathore S. Cone-beam CT diagnostic applications: caries, periodontal bone assessment, and endodontic applications. Dent Clin North Am 2008;52(4):825–841, vii.
3. Tonetti MS. Periodontitis and risk for atherosclerosis: an update on intervention trials. J Clin Periodontol 2009;36(Suppl 10):15–19.
4. Chen L, Wei B, Li J, et al. Association of periodontal parameters with metabolic level and systemic inflammatory markers in patients with type 2 diabetes. J Periodontol 2010;81(3):364–371.
5. Grössner-Schreiber B, Fetter T, Hedderich J, Kocher T, Schreiber S, Jepsen S. Prevalence of dental caries and periodontal disease in patients with inflammatory bowel disease: a case-control study. J Clin Periodontol 2006;33(7):478–484.
6. Loesche W. Dental caries and periodontitis: contrasting two infections that have medical implications. Infect Dis Clin North Am 2007;21(2):471–502, vii.
7. Miracle AC, Mukherji SK. Conebeam CT of the head and neck: part 1—physical principles. AJNR Am J Neuroradiol 2009;30(6):1088–1095.

8. Yamashina A, Tanimoto K, Sutthiprapaporn P, Hayakawa Y. The reliability of computed tomography (CT) values and dimensional measurements of the oropharyngeal region using cone beam CT: comparison with multidetector CT. Dentomaxillofac Radiol 2008;37(5):245–251.
9. White SC, Pharoah MJ. The evolution and application of dental maxillofacial imaging modalities. Dent Clin North Am 2008;52(4):689–705, v.
10. Scholl RJ, Kellett HM, Neumann DP, Lurie AG. Cysts and cystic lesions of the mandible: clinical and radiologic-histopathologic review. RadioGraphics 1999;19(5):1107–1124.
11. Dunfee BL, Sakai O, Pistey R, Gohel A. Radiologic and pathologic characteristics of benign and malignant lesions of the mandible. RadioGraphics 2006; 26(6):1751–1768.
12. DelBalso AM. Lesions of the jaws. Semin Ultrasound CT MR 1995;16(6):487–512.
13. Abrahams JJ. Dental CT imaging: a look at the jaw. Radiology 2001;219(2):334–345.
14. Abrahams JJ, Berger SB. Inflammatory disease of the jaw: appearance on reformatted CT scans. AJR Am J Roentgenol 1998;170(4):1085–1091.
15. Huumonen S, Ørstavik D. Radiological aspects of apical periodontitis. Endod Top 2002;1(1):3–25.
16. Abrahams JJ, Glassberg RM. Dental disease: a frequently unrecognized cause of maxillary sinus abnormalities? AJR Am J Roentgenol 1996;166(5): 1219–1223.
17. Kretzschmar DP, Kretzschmar JL. Rhinosinusitis: review from a dental perspective. Oral Surg Oral Med Oral Pathol Oral Radiol Endod 2003;96(2):128–135.
18. El Nesr NM, Avery JK. Tooth eruption and shedding. In: Avery JK, Steele PF, Avery N, eds. Oral development and histology. 3rd ed. Stuttgart, Germany: Thieme, 2002; 123–140.
19. Wright JT. Normal formation and development defects of the human dentition. Pediatr Clin North Am 2000;47(5):975–1000.
20. Gard N, Garg A. Textbook of operative dentistry. New Delhi, India: JP Medical, 2010.
21. Goske MJ, Applegate KE, Boylan J, et al. The Image Gently campaign: working together to change practice. AJR Am J Roentgenol 2008;190(2):273–274.
22. Brink JA, Amis ES Jr. Image Wisely: a campaign to increase awareness about adult radiation protection. Radiology 2010;257(3):601–602.
23. Rajab LD, Hamdan MA. Supernumerary teeth: review of the literature and a survey of 152 cases. Int J Paediatr Dent 2002;12(4):244–254.
24. Anthonappa RP, Lee CK, Yiu CK, King NM. Hypohyperdontia: literature review and report of seven cases. Oral Surg Oral Med Oral Pathol Oral Radiol Endod 2008;106(5):e24–e30.
25. Russell KA, Folwarczna MA. Mesiodens: diagnosis and management of a common supernumerary tooth. J Can Dent Assoc 2003;69(6):362–366.
26. Harris EF, Clark LL. An epidemiological study of hyperdontia in American blacks and whites. Angle Orthod 2008;78(3):460–465.
27. Grimanis GA, Kyriakides AT, Spyropoulos ND. A survey on supernumerary molars. Quintessence Int 1991;22(12):989–995.
28. Reichart PA, Philipsen HP. Color atlas of oral pathology. Stuttgart, Germany: Thieme, 2000; 222–249.
29. Krennmair G, Lenglinger FX, Traxler M. Imaging of unerupted and displaced teeth by cross-sectional CT scans. Int J Oral Maxillofac Surg 1995;24(6): 413–416.
30. Kokich VG. Surgical and orthodontic management of impacted maxillary canines. Am J Orthod Dentofacial Orthop 2004;126(3):278–283.
31. Barrett JF, Keat N. Artifacts in CT: recognition and avoidance. RadioGraphics 2004;24(6):1679–1691.
32. Mitchell DA, Mitchell L. Oxford handbook of clinical dentistry. New York, NY: Oxford University Press, 2005; 23–52.
33. Sidhu SK. Glass-ionomer cement restorative materials: a sticky subject? Aust Dent J 2011;56 (Suppl 1):23–30.
34. Odlum O. A method of eliminating streak artifacts from metallic dental restorations in CTs of head and neck cancer patients. Spec Care Dentist 2001; 21(2):72–74.
35. Metzger Z, Abramovitz I, Bergenholtz G. Apical periodontitis. In: Bergenholtz G, Horsted-Bindslev P, Reit C, eds. Textbook of endodontology. Oxford, England: Blackwell, 2003; 113–126.
36. Le A, Shetty V. Normal wound healing. In: Andersson L, Kahnberg KE, Pogrel MA, eds. Oral and maxillofacial surgery. West Sussex, England: Blackwell, 2010; 165–169.
37. Abrahams JJ, Berger SB. Oral-maxillary sinus fistula (oroantral fistula): clinical features and findings on multiplanar CT. AJR Am J Roentgenol 1995;165(5):1273–1276.
38. Craddock HL, Youngson CC. A study of the incidence of overeruption and occlusal interferences in unopposed posterior teeth. Br Dent J 2004;196(6):341–348; discussion 337.
39. Arai I, Aoki T, Yamazaki H, Ota Y, Kaneko A. Pneumomediastinum and subcutaneous emphysema after dental extraction detected incidentally by regular medical checkup: a case report. Oral Surg Oral Med Oral Pathol Oral Radiol Endod 2009;107(4):e33–e38.
40. Sekine J, Irie A, Dotsu H, Inokuchi T. Bilateral pneumothorax with extensive subcutaneous emphysema manifested during third molar surgery: a case report. Int J Oral Maxillofac Surg 2000;29 (5):355–357.
41. Tang L, Zhou XD, Wang Y, Zhang L, Zheng QH, Huang DM. Detection of vertical root fracture using cone beam computed tomography: report of two cases. Dent Traumatol 2011;27(6):484–488.
42. Trope M. Avulsion of permanent teeth: theory to practice. Dent Traumatol 2011;27(4):281–294.
43. Molloy S. Microbiome: tipping the balance. Nat Rev Microbiol 2012;10(1):3.
44. Anbiaee N, Tafakhori Z. Early diagnosis of progressive systemic sclerosis (scleroderma) from a panoramic view: report of three cases. Dentomaxillofac Radiol 2011;40(7):457–462.
45. Givol N, Buchner A, Taicher S, Kaffe I. Radiological features of osteogenic sarcoma of the jaws: a comparative study of different radiographic modalities. Dentomaxillofac Radiol 1998;27(6):313–320.
46. Fragiskos FD. Odontogenic infections. In: Fragiskos FD, ed. Oral surgery. Berlin, Germany: Springer-Verlag, 2007; 205–241.
47. Ohshima A, Ariji Y, Goto M, et al. Anatomical considerations for the spread of odontogenic infection originating from the pericoronitis of impacted mandibular third molar: computed tomographic analyses. Oral Surg Oral Med Oral Pathol Oral Radiol Endod 2004;98(5):589–597.

48. Ness GM, Peterson LJ. Impacted teeth. In: Miloro M, Ghali GE, Larsen P, Waite P, eds. Peterson's principles of oral and maxillofacial surgery. 2nd ed. Hamilton, Ontario: Decker, 2004.
49. Murray JJ, Rugg-Gunn AJ, Jenkins GN. Fluorides in caries prevention. 3rd ed. Oxford, England: Butterworth-Heinemann, 1991.
50. Tymofiyeva O, Boldt J, Rottner K, Schmid F, Richter EJ, Jakob PM. High-resolution 3D magnetic resonance imaging and quantification of carious lesions and dental pulp in vivo. MAGMA 2009;22(6):365–374.
51. Stookey GK. The effect of saliva on dental caries. J Am Dent Assoc 2008;139(Suppl):11S–17S.
52. Soto-Rojas AE, Kraus A. The oral side of Sjögren syndrome: diagnosis and treatment—a review. Arch Med Res 2002;33(2):95–106.
53. Garg AK, Malo M. Manifestations and treatment of xerostomia and associated oral effects secondary to head and neck radiation therapy. J Am Dent Assoc 1997;128(8):1128–1133.
54. Silva AR, Alves FA, Antunes A, Goes MF, Lopes MA. Patterns of demineralization and dentin reactions in radiation-related caries. Caries Res 2009; 43(1):43–49.
55. Lin LM, Huang GTJ. Pathobiology of the periapex. In: Hargreaves KM, Cohen S, eds. Cohen's pathways of the pulp. 10th ed. New York, NY: Mosby, 2011; 529–558.
56. Alexandridis C. Surgical treatment of radicular cysts. In: Fragiskos FD, ed. Oral surgery. Berlin, Germany: Springer-Verlag, 2007; 301–308.
57. Lesmes D, Laster Z. Innovations in dental implant design for current therapy. Oral Maxillofac Surg Clin North Am 2011;23(2):193–200, v.
58. Pace R, Cairo F, Giuliani V, Prato LP, Pagavino G. A diagnostic dilemma: endodontic lesion or odontogenic keratocyst? A case presentation. Int Endod J 2008;41(9):800–806.
59. Wood NK. Periapical lesions. Dent Clin North Am 1984;28(4):725–766.
60. Ricucci D, Mannocci F, Ford TR. A study of periapical lesions correlating the presence of a radiopaque lamina with histological findings. Oral Surg Oral Med Oral Pathol Oral Radiol Endod 2006; 101(3):389–394.
61. Carrillo C, Penarrocha M, Ortega B, Martí E, Bagán JV, Vera F. Correlation of radiographic size and the presence of radiopaque lamina with histological findings in 70 periapical lesions. J Oral Maxillofac Surg 2008;66(8):1600–1605.
62. Trope M, Pettigrew J, Petras J, Barnett F, Tronstad L. Differentiation of radicular cyst and granulomas using computerized tomography. Endod Dent Traumatol 1989;5(2):69–72.
63. Aggarwal V, Logani A, Shah N. The evaluation of computed tomography scans and ultrasounds in the differential diagnosis of periapical lesions. J Endod 2008;34(11):1312–1315.
64. Orstavik D. Time-course and risk analyses of the development and healing of chronic apical periodontitis in man. Int Endod J 1996;29(3):150–155.
65. Holly D, Jurkovic R, Mracna J. Condensing osteitis in oral region. Bratisl Lek Listy (Tlacene Vyd) 2009;110(11):713–715.
66. Kerr AR, Phelan JA. Benign lesions of the oral cavity. In: Burket LW, Greenberg MS, Glick M, Ship JA, eds. Burket's oral medicine. 11th ed. Hamilton, Ontario: Decker, 2008; 129–152.
67. Venkatesh KV, Nandini VV. Periapical radiolucency not requiring endodontic therapy: an unusual case. Indian J Dent Res 2009;20(1):126–128.
68. Mehra P, Murad H. Maxillary sinus disease of odontogenic origin. Otolaryngol Clin North Am 2004;37(2):347–364.
69. Brook I. Microbiology of acute and chronic maxillary sinusitis associated with an odontogenic origin. Laryngoscope 2005;115(5):823–825.
70. Falk H, Ericson S, Hugoson A. The effects of periodontal treatment on mucous membrane thickening in the maxillary sinus. J Clin Periodontol 1986; 13(3):217–222.
71. Patel NA, Ferguson BJ. Odontogenic sinusitis: an ancient but under-appreciated cause of maxillary sinusitis. Curr Opin Otolaryngol Head Neck Surg 2012;20(1):24–28.
72. Brook I. Sinusitis of odontogenic origin. Otolaryngol Head Neck Surg 2006;135(3):349–355.
73. Hansen JG, Højbjerg T, Rosborg J. Symptoms and signs in culture-proven acute maxillary sinusitis in a general practice population. APMIS 2009;117 (10):724–729.
74. Baykul T, Doğru H, Yasan H, Cina Aksoy M. Clinical impact of ectopic teeth in the maxillary sinus. Auris Nasus Larynx 2006;33(3):277–281.
75. Yonetsu K, Izumi M, Nakamura T. Deep facial infections of odontogenic origin: CT assessment of pathways of space involvement. AJNR Am J Neuroradiol 1998;19(1):123–128.
76. Kim HJ, Park ED, Kim JH, Hwang EG, Chung SH. Odontogenic versus nonodontogenic deep neck space infections: CT manifestations. J Comput Assist Tomogr 1997;21(2):202–208.
77. Obayashi N, Ariji Y, Goto M, et al. Spread of odontogenic infection originating in the maxillary teeth: computerized tomographic assessment. Oral Surg Oral Med Oral Pathol Oral Radiol Endod 2004;98 (2):223–231.
78. Mehra P, Caiazzo A, Bestgen S. Odontogenic sinusitis causing orbital cellulitis. J Am Dent Assoc 1999;130(7):1086–1092.
79. Caruso PA, Watkins LM, Suwansaard P, et al. Odontogenic orbital inflammation: clinical and CT findings—initial observations. Radiology 2006; 239(1):187–194.
80. Sakamoto H, Aoki T, Kise Y, Watanabe D, Sasaki J. Descending necrotizing mediastinitis due to odontogenic infections. Oral Surg Oral Med Oral Pathol Oral Radiol Endod 2000;89(4):412–419.
81. Som PM, Curtin HD. Fascia and spaces of the neck. In: Som PM, Curtin HD, eds. Head and neck imaging. 4th ed. St Louis, Mo: Mosby, 2003; 1805–1827.
82. Rana RS, Moonis G. Head and neck infection and inflammation. Radiol Clin North Am 2011;49(1): 165–182.
83. Osborn TM, Assael LA, Bell RB. Deep space neck infection: principles of surgical management. Oral Maxillofac Surg Clin North Am 2008;20(3): 353–365.

Teeth: What Radiologists Should Know

Meir H. Scheinfeld, MD, PhD • Keivan Shifteh, MD • Laura L. Avery, MD Harry Dym, DDS • R. Joshua Dym, MD

RadioGraphics 2012; 32:1927–1944 • **Published online** 10.1148/rg.327125717 • **Content Codes:** CT HN NR

Page 1928
When interpreting multidetector computed tomographic (CT) images, the radiologist may provide added value by identifying definite or possible dental lesions and referring the patient to a dental specialist for clinical evaluation and dedicated radiography or cone-beam CT, as necessary (2).

Page 1934
In periodontitis, bone loss occurs between teeth and at the furcations between roots, thereby uncovering the tooth roots, which are normally covered by the bone of the alveolar processes (Fig 12).

Page 1937
Early carious lesions commonly have a mushroom shape, with the "stalk" representing a narrow channel through the enamel and the "head" representing a larger area of dentin demineralization undermining the enamel. Lesions in the anterior teeth and advanced lesions in the posterior teeth are more ovoid.

Page 1937
Apical periodontitis refers to a spectrum of diseases that occur around the tooth apex, including periapical granuloma, periapical abscess, and periapical (radicular) cyst (35,55).

Page 1940
The relationship between the teeth and the maxillary sinus is best seen on sagittal and coronal images (Fig 17) (16). Sinus mucosal thickening associated with focal ballooning or dehiscence of the floor of the maxillary sinus above a carious tooth is highly suspicious for an odontogenic source of infection.